

Magnetic and Optical Properties of LiNbO_3
Type InCoO_3 and InFeO_3 perovskite
materials.

COURSE CODE : TP-407

SUBMITTED BY

CLASS ROLL : FH-098-036 EXAM ROLL: 30214

REGISTRATION NUMBER : 2016-514-722

SESSION : 2016-17



DEPARTMENT OF THEORETICAL PHYSICS

UNIVERSITY OF DHAKA

March 24, 2022

Contents

1	Abstract	4
2	Introduction	4
3	Computaion Method	8
4	Results	13
5	Conclusion	23

List of Figures

1	Cubic Structure of InCoO3	5
2	Cubic Structure of InFeO3	6
3	X-Ray diffraction pattern of InCoO3	6
4	X-Ray diffraction pattern of InFeO3	7
5	Band Structure Of InCoO3	12
6	Band Structure Of InFeO3	13
7	Density of States Of InCoO3	14
8	Density of States Of InFeO3	15
9	Absorption Of InCoO3 and InFeO3	16
10	Reflectivity Of InCoO3 and InFeO3	17
11	Dielectric constants of InCoO3 and InFeO3(Real)	18
12	Dielectric constants of InCoO3 and InFeO3(Imaginary)	19
13	Optical Conductivity of InCoO3 and InFeO3(Real)	20
14	Optical Conductivity of InCoO3 and InFeO3(Imaginary)	21
15	Extinction graph of INCoO3 and InFeO3	22
16	Energyloss spectrum of InCoO3 and InFeO3	23

1 Abstract

Metal oxide perovskites are increasingly popular for magnetic and optoelectronic applications in industrial purposes. In this study, structural magnetic and optical properties of InCoO_3 , and InFeO_3 were unearthed using the first principles of density functional theory. These materials exhibit semiconducting behavior with indirect bandgap energy. The high absorption coefficient, low reflectivity, and high optical conductivity make them suitable for photovoltaic and other optoelectronic and memory device applications. Among them, InFeO_3 is more favorable for magnetic and optical applications.

2 Introduction

The use of solar energy to catalyze photo-driven operations has attracted enormous engagement from the scientific society because of its great potential to handle energy and environmental issues. In this regard, several attempts have been made by researchers to design and develop different materials with enhanced photocatalytic efficiencies.[1]

Perovskite, named after the Russian mineralogist L.A. Perovski, has a specific crystal structure with the ABX_3 formula ($X = \text{oxygen, halogen}$). The larger A cation occupies a cubo-octahedral site shared with twelve X anions while the smaller B cation is stabilized in an octahedral site shared with six X anions. The most studied perovskites are oxides due to their electrical properties of ferroelectricity or superconductivity. Halide perovskites

received little attention until layered organometal halide perovskites were reported to exhibit a semiconductor-to-metal transition with increasing dimensionality. In a quest for nanoparticles, solar cells, and enhanced optical and magnetic properties, perovskite materials suit flawlessly in that range [1]. Perovskite materials contain properties like tunable bandgap, long charge diffusion length, good charge carrier mobility, low carrier recombination rate, high dielectric constant. They have high efficiency in photoconductor-based X-ray detectors, spectroscopy, acoustic wave signal processing, and image storage device. These materials are the class of material that bears the chemical structure of ABO_3 [2, 3, 4].

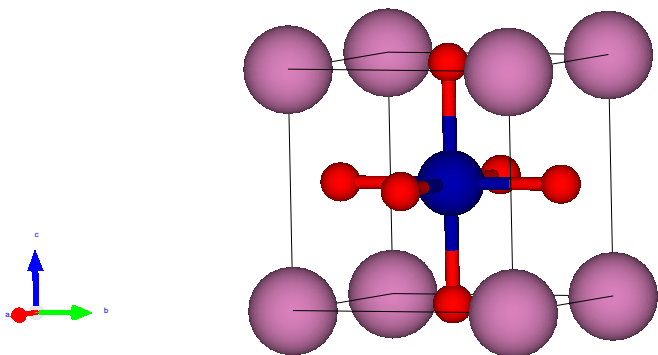


Figure 1: Cubic Structure of InCoO3

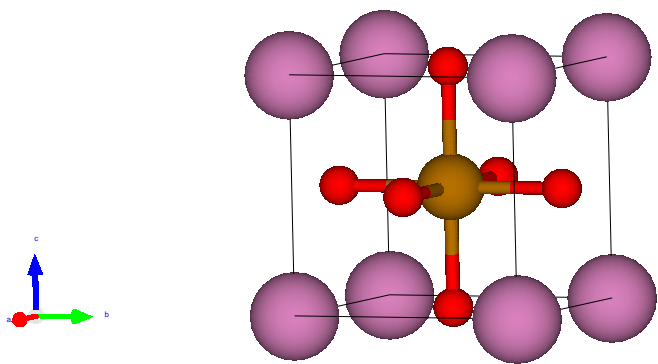


Figure 2: Cubic Structure of InFeO_3

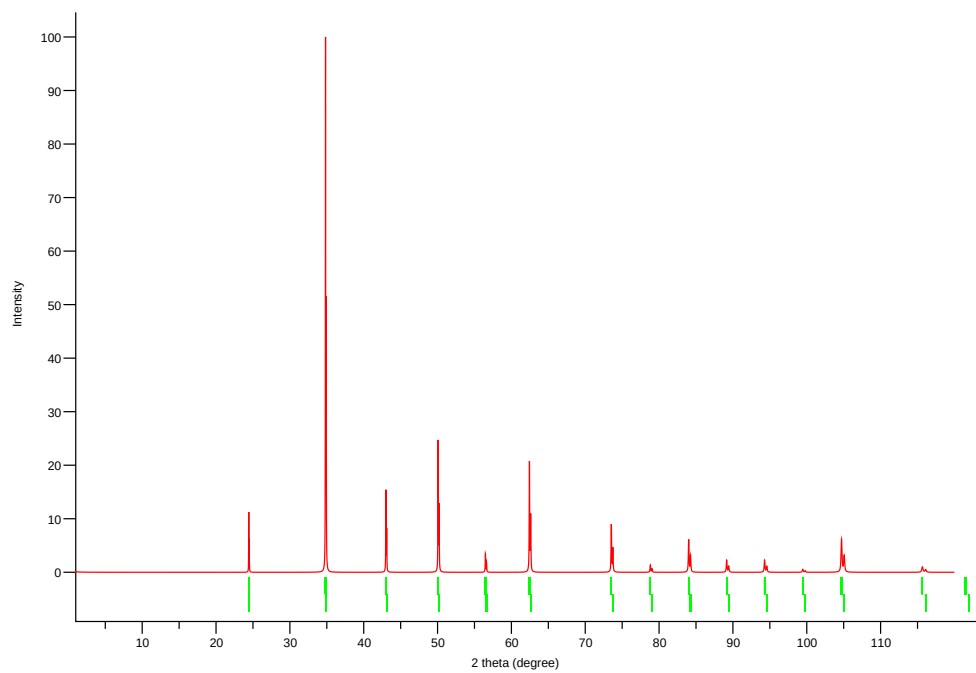


Figure 3: X-Ray diffraction pattern of InCoO_3

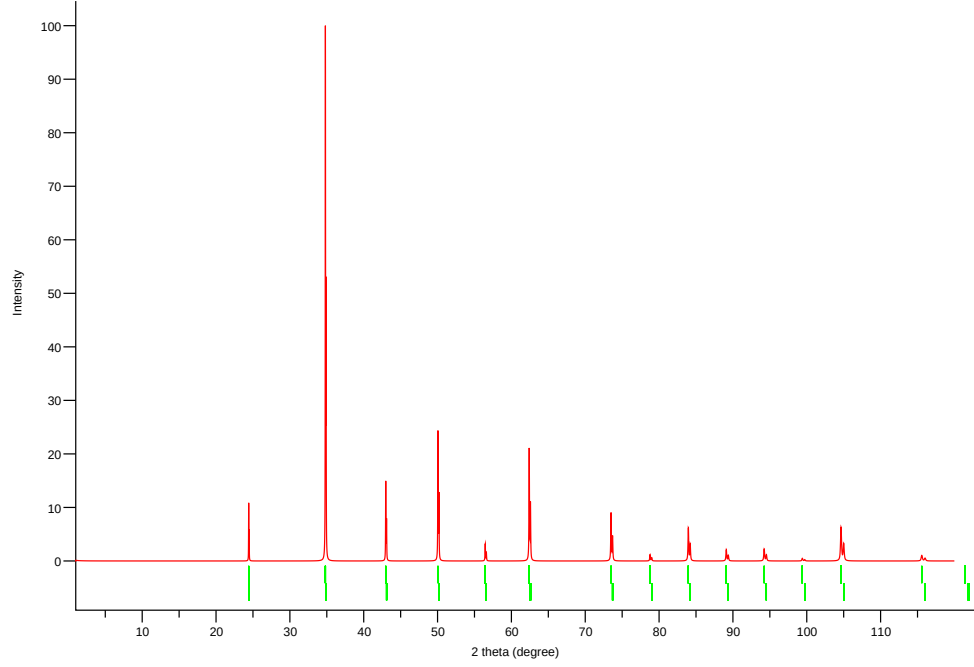


Figure 4: X-Ray diffraction pattern of InFeO₃

In this type of material, O is oxygen with (-2) ionic valence anion, and A and B metal cations give (+6) valence ion combined. Perovskite material family has numerous types of oxide form like transition metal oxides with the general formula of ABO₃[2]. One perovskite material is LiNbO₃. For that, we took LiNbO₃-like material InCoO₃, InFeO₃ and sampled magnetic and optical properties with DFT calculations[5].

3 Computaion Method

During the past decade, computer simulations based on a quantum-mechanical description of the interactions between electrons and between electrons and atomic nuclei have developed an increasingly important impact on solid-state physics and chemistry and on materials science—promoting not only a deeper understanding, but also the possibility to contribute significantly to materials design for future technologies. This development is based on two important columns:

- (i) The improved description of electronic many-body effects within density-functional theory (DFT) and the upcoming post-DFT methods.
- (ii) The implementation of the new functionals and many-body techniques within highly efficient, stable, and versatile computer codes, which allow to exploit the potential of modern computer architectures.

An understanding of mathematical functions and functionals is required to understand the basic language of DFT[6]. Functions take a number as input and yield a number as output. For example, eq 1, could take $x = 2$ as input and yield $f(x) = 4$ as output. Functionals are functions of functions. Functionals take a function as input and yield a number as output. The input for a function is enclosed in parentheses (for example $f(x)$), whereas the input for a functional is enclosed in square brackets (for example $F[y]$).

A very simple functional is the definite integral functional, $F[y]$ that yields the area under any provided function, y . For example, let us say that we are interested in the area under any general curve, $y = f(x)$, from $x = 0$ to $x = 3$. The functional, $F[y]$, is then given by

$$y = f(x) = 2x \tag{1}$$

$$F[y] = \int_0^3 f(x)dx \tag{2}$$

The functional $F[y]$ in eq 2 could take the function given in eq 1 as input and yield the output $F[2x] = 9$. Functionals can be defined as either local or nonlocal. A functional is local if the functional's value can be computed for small segments of the input curve and then summed to find the total value. Otherwise the functional is called nonlocal. A density functional takes the electron density (a function of the position coordinate, r) as an input and outputs a number (an energy). Density functionals can be local or nonlocal.

As usual in many-body electronic structure calculations, the nuclei of the treated molecules or clusters are seen as fixed (the Born–Oppenheimer approximation), generating a static external potential V , in which the electrons are moving. A stationary electronic state is then described by a wavefunction $\psi(r_1, \dots, r_N)$ satisfying the many-electron time-independent

Schrödinger equation.

$$\begin{aligned}\hat{H}\Psi &= [\hat{T} + \hat{V} + \hat{U}] \\ &= \left[\sum_{i=1}^N \left(-\frac{\hbar}{2m_i} \Delta_i^2 \right) + \sum_{i=1}^N V(r_i) + \sum_{i<j}^N U(r_i, r_j) \right] \Psi = E\Psi\end{aligned}\quad (3)$$

where, for the N-electron system, \hat{H} is the Hamiltonian, E is the total energy, \hat{T} is the kinetic energy, \hat{V} is the potential energy from the external field due to positively charged nuclei, and \hat{U} is the electron-electron interaction energy. As $\hat{T}\hat{U}$ is equal for any N-electron system, they are called universal operator. Only \hat{V} is system-dependent. This complicated many-particle equation is not detachable into simpler single-particle equations because of the interaction term \hat{U} . There are numerous cultivated processes for translating the many-body Schrödinger equation based on the development of the wavefunction in Slater determinants. While the easiest one is the Hartree-Fock method, more cultivated techniques are usually tagged as post-Hartree-Fock methods. Nevertheless, the problem with these scenarios is the huge computational effort, which renders it practically incompressible to apply them efficiently to more considerable, more complex techniques. separable. Here DFT supplies an adorable alternative, being vastly more universal, as it supplies a way to systematically map the many-body issue, with \hat{U} , onto a single-body problem without \hat{U} , onto a single-body problem without \hat{U} . In DFT the key variable is the electron density $n(\mathbf{r})$, which for a normalized Ψ is given by

$$n(r) = N \int d^3r_2 \dots \int d^3r_N \Psi^*(r_1, r_2, \dots, r_n) \Psi(r_1, r_2, \dots, r_n) \quad (4)$$

In this review, I discuss the implementation of various DFT functionals [local-density approximation (LDA), generalized gradient approximation (GGA), meta-GGA, hybrid functional mixing DFT, and exact (Hartree-Fock) exchange] and post-DFT approaches [DFT + U for strong electronic correlations in narrow bands, many-body perturbation theory (GW) for quasi-particle spectra, dynamical correlation effects via the adiabatic-connection fluctuation-dissipation theorem (AC-FDT)] in the Vienna ab initio simulation package VASP.

For computing the magnetic and optical properties of InFeO₃ and InCoO₃, we execute Density Functional Theory (DFT)[7, 8, 9, 10] simulations by Vienna ab initio Simulation Package (VASP)[11, 12, 13]. The unit cells of InCoO₃ and InFeO₃ in the cubic form are shown in Fig. 1, which we explored further. First, we perform structural relaxation. Then we execute static calculation for density of states, band, and optical properties of chosen materials.

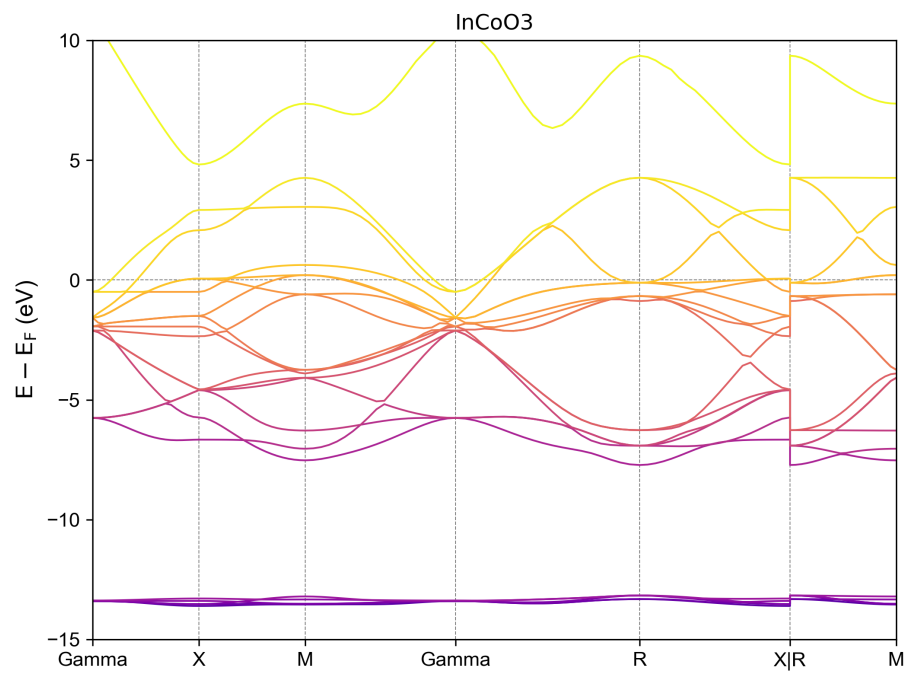


Figure 5: Band Structure Of InCoO3

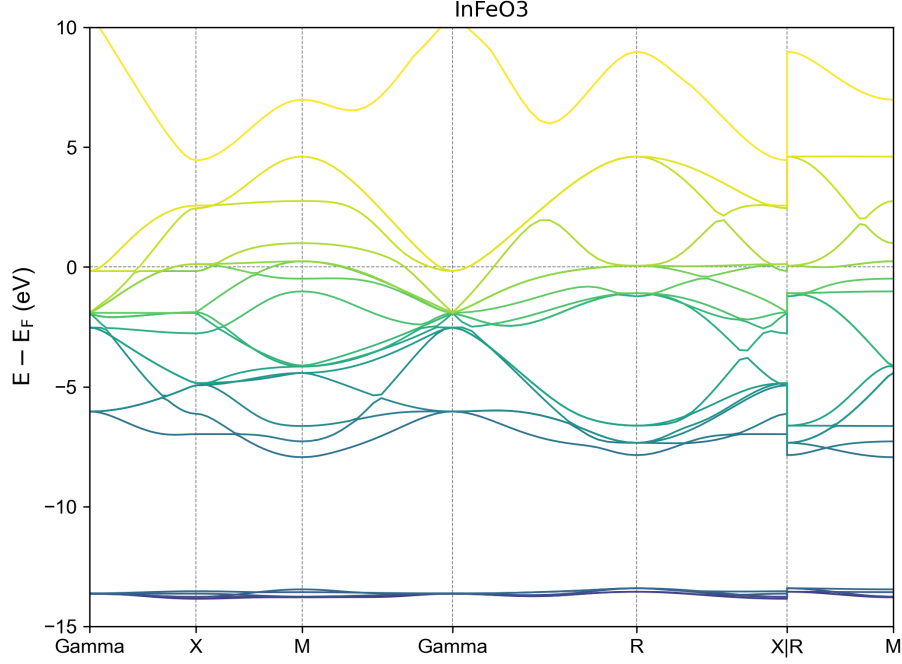


Figure 6: Band Structure Of InFeO3

4 Results

InFeO3 and InCoO3 are cubic structures under the space group of Pm3m (no. 221). We visualize the structures in VESTA (3D Visualization for Electronic and Structural Analysis). The unit cell of InCoO3 and InFeO3 constitutes five atoms (shown in Fig. 1). Fe or Co atoms hold the corner positions of the cubes (Wyckoff site (0,0,0)), In situated in the crystal's body-centered positions (Wyckoff site(0.5,0.5,0.5)). O occupies face-centered positions (Wyckoff site (0.5,0.5,0)). The electronic band structures and den-

sity of states(DOS) of relaxed InCoO3 and InFeO3 structures through PBE functional considering the GGA approximation. Band structures of InCoO3 and InFeO3 are shown in Fig. 2.

Zero-point energy is Fermi energy. Two structures show indirect bandgap and the range of the bandgap energy resembles that both the structures are metallic in nature. The outcome of the bandgaps and band structures of the examined materials confirm their wonder for photothermal, photovoltaic, and optoelectronic applications. InCoO3 and InFeO3 show the same bandgap. The density of states of atoms is shown in Fig. 3.

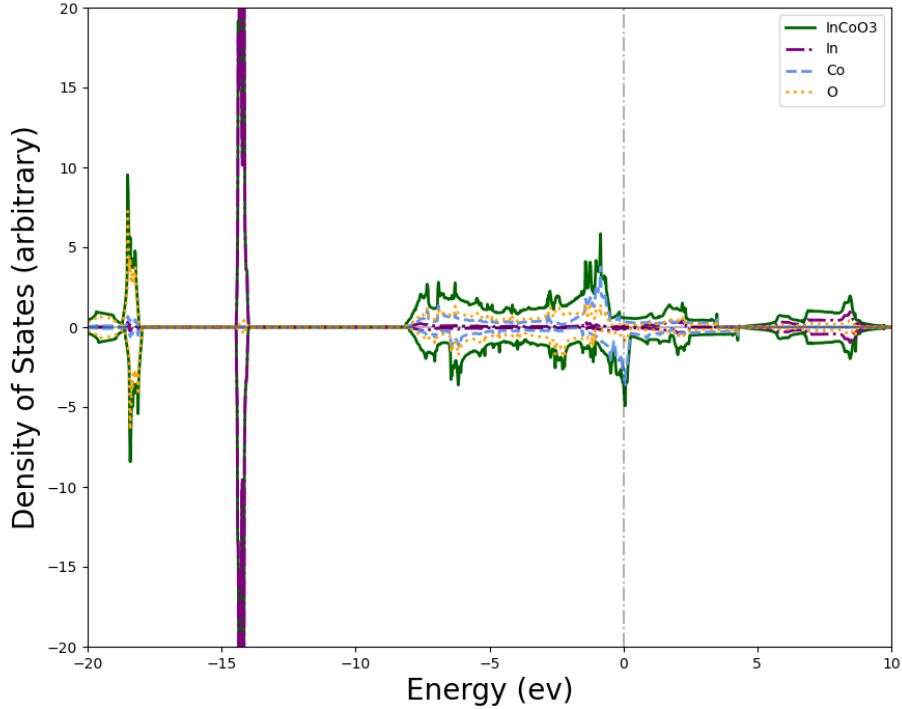


Figure 7: Density of States Of InCoO3

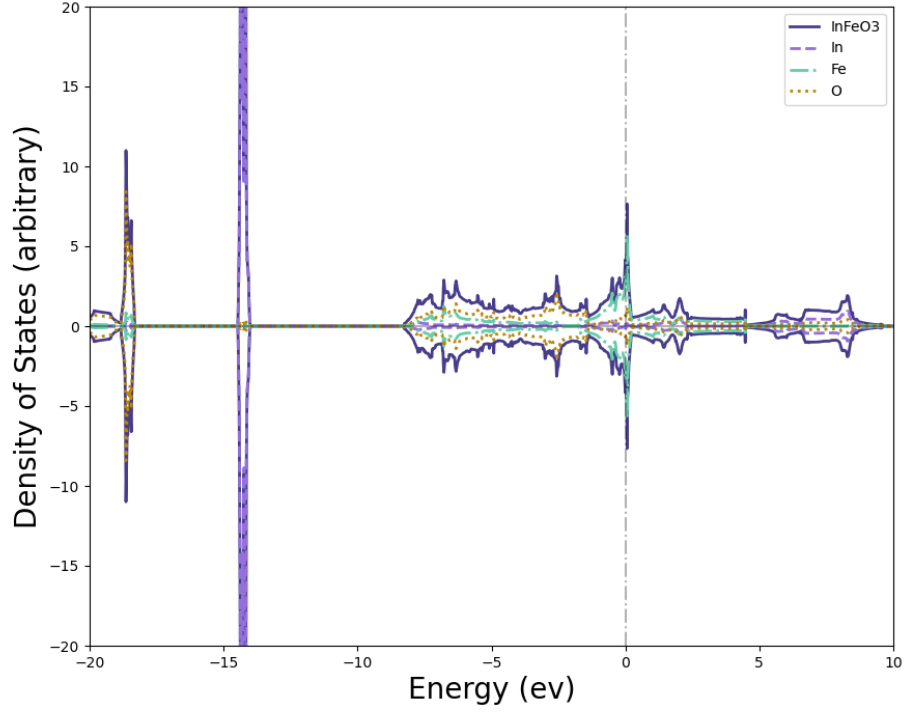


Figure 8: Density of States Of InFeO3

The orbital projected density of states indicates at the Fermi level, the p-orbital of Co and Fe atom is the main benefactor. The optical properties of a material rely on many parts. Such as absorption spectra, concerning light energy and wavelength, reflectivity, refractivity index, dielectric constants, and optical conductivity. We examined these properties with InCoO3 and InFeO3. The optical absorption coefficient indicates how much light penetrates the substance before being absorbed by the material. This is a piece of important knowledge for solar-energy conversion efficiency for practical application. In Fig. 4 energy and wavelength-dependent absorption profiles

are demonstrated.

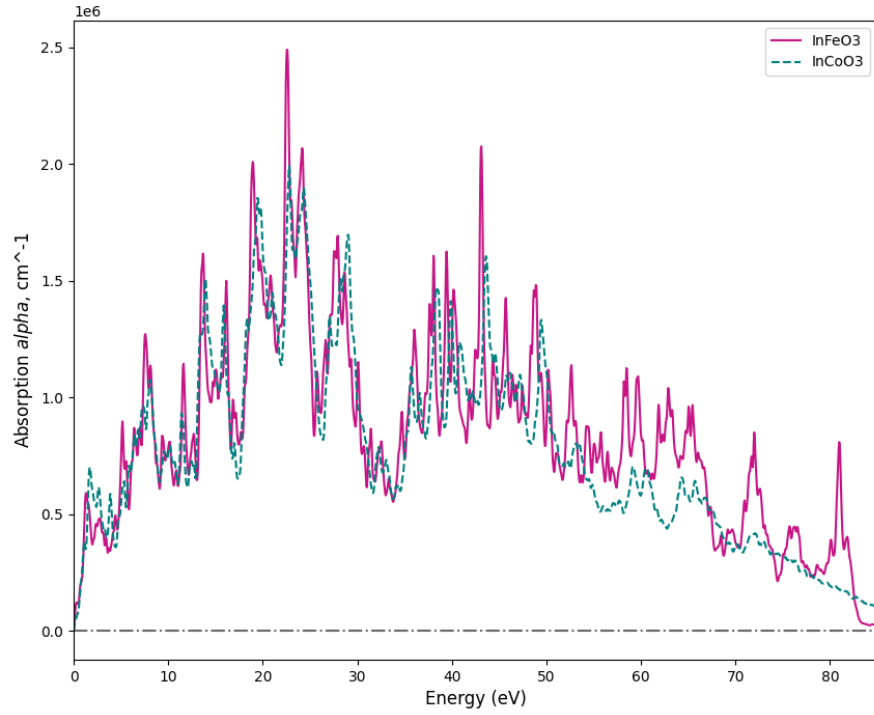


Figure 9: Absorption Of InCoO3 and InFeO3

Reflectivity is an optical property to understand the surface nature of the material. It defines how much energy reflects from incident energy on the surface. Fig 5 represents the optical reflectivity of InCoO3 and InFeO3.

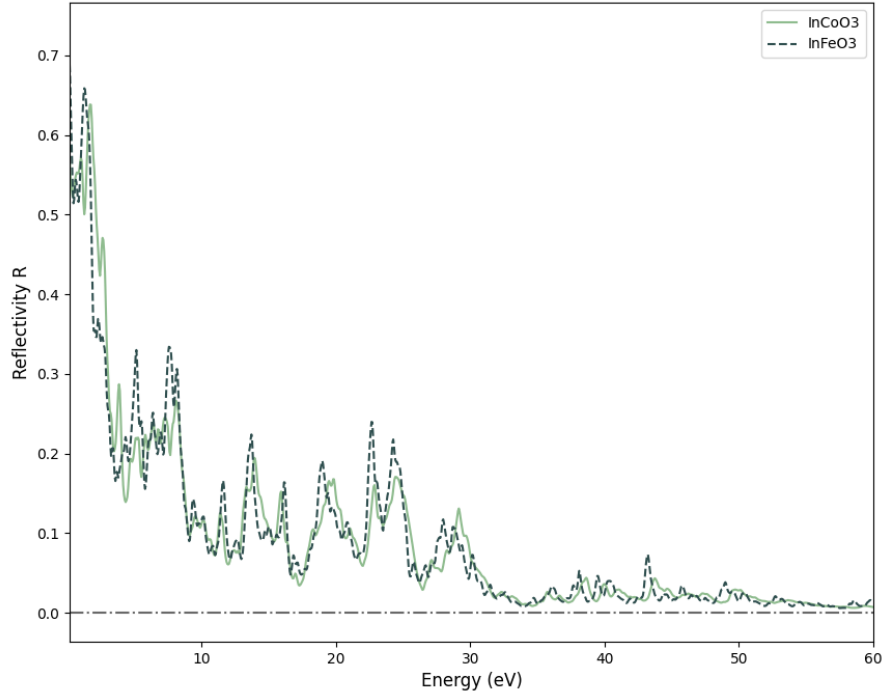


Figure 10: Reflectivity Of InCoO3 and InFeO3

The dielectric constant values are used for determining how well optoelectronic devices work, defined as the response of a material to incident light energy. Higher dielectric values at a lower charge carrier recombination rate are deep in improving the optoelectronic device performance.

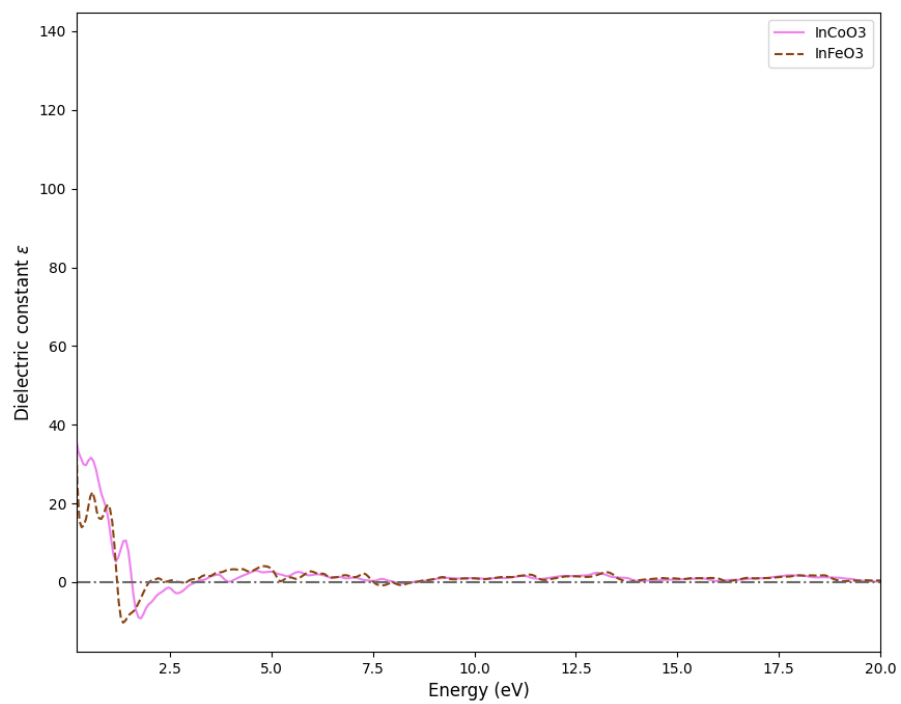


Figure 11: Dielectric constants of InCoO3 and InFeO3(Real)

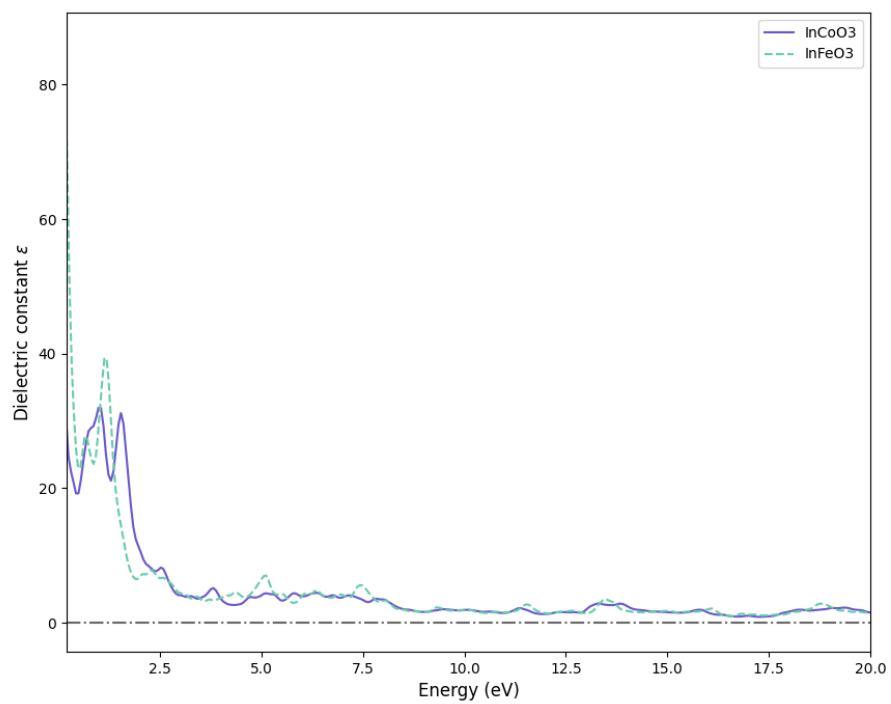


Figure 12: Dielectric constants of InCoO3 and InFeO3(Imaginary)

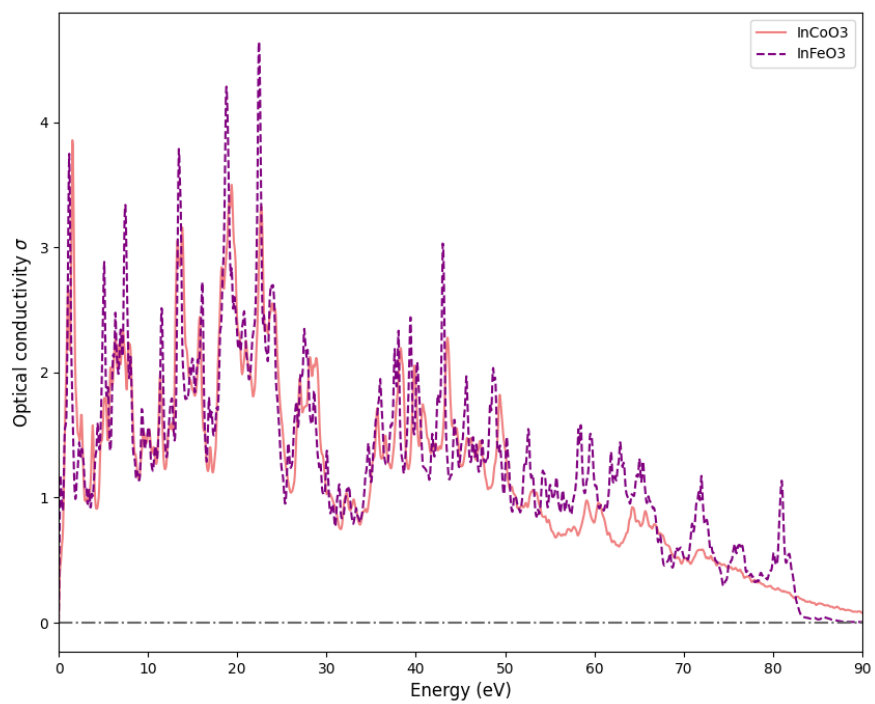


Figure 13: Optical Conductivity of InCoO3 and InFeO3(Real)

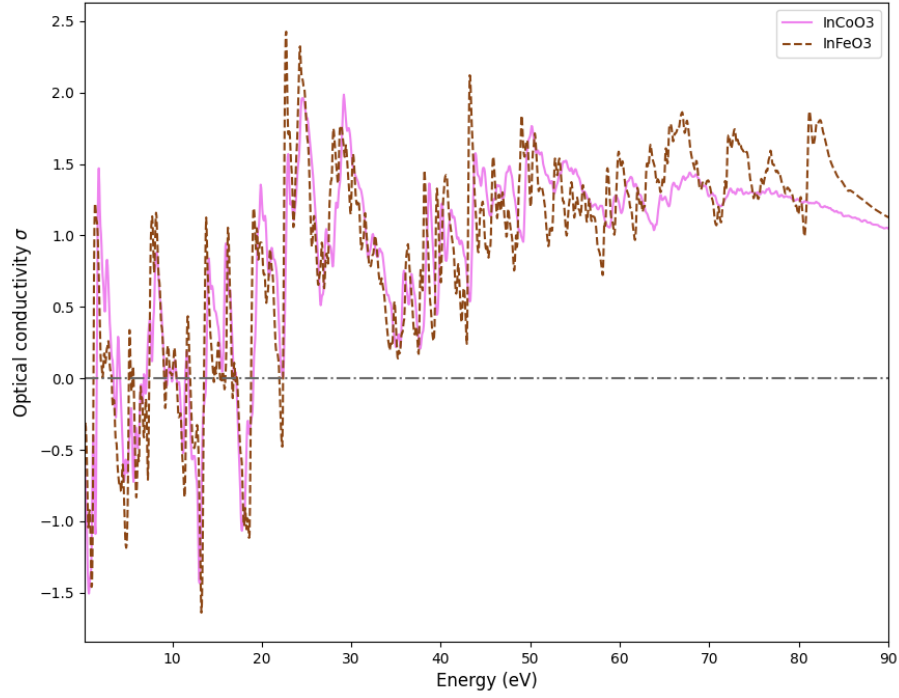


Figure 14: Optical Conductivity of InCoO3 and InFeO3(Imaginary)

The optical conductivity of a material specifies the electric conductivity of a photon from electromagnetic absorption. Fig 6 shows the dielectric constants of InCoO3 and InFeO3. Fig 7 shows us optical conductivity between InCoO3 and InFeO3. Fig. 9 and 10 shows Extinction and Energuloss spectrum of InCoO3 and InFeO3 graph respectively.

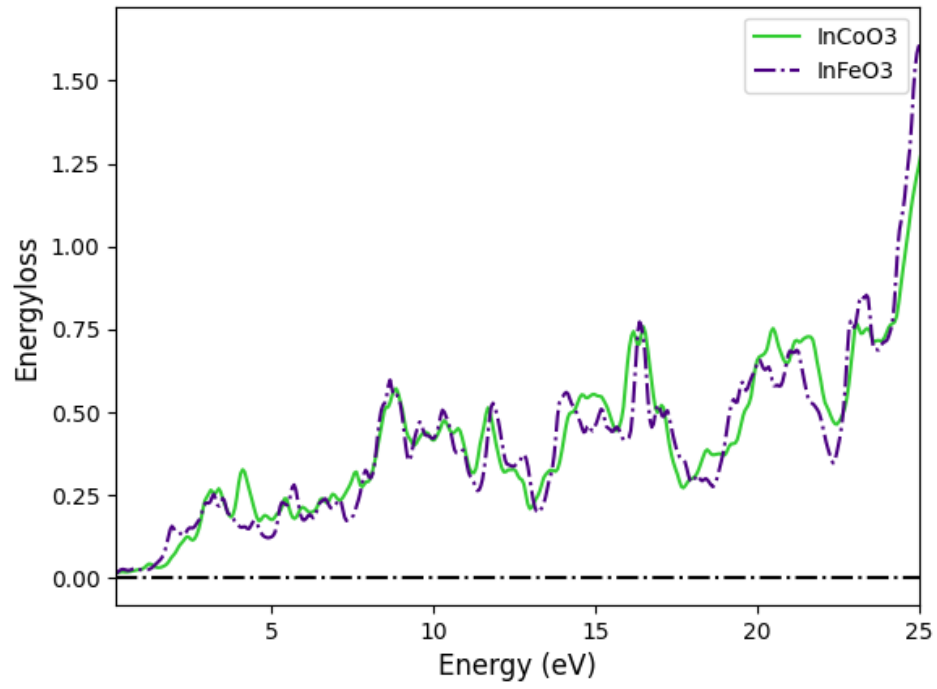


Figure 15: Extinction graph of INCoO3 and InFeO3

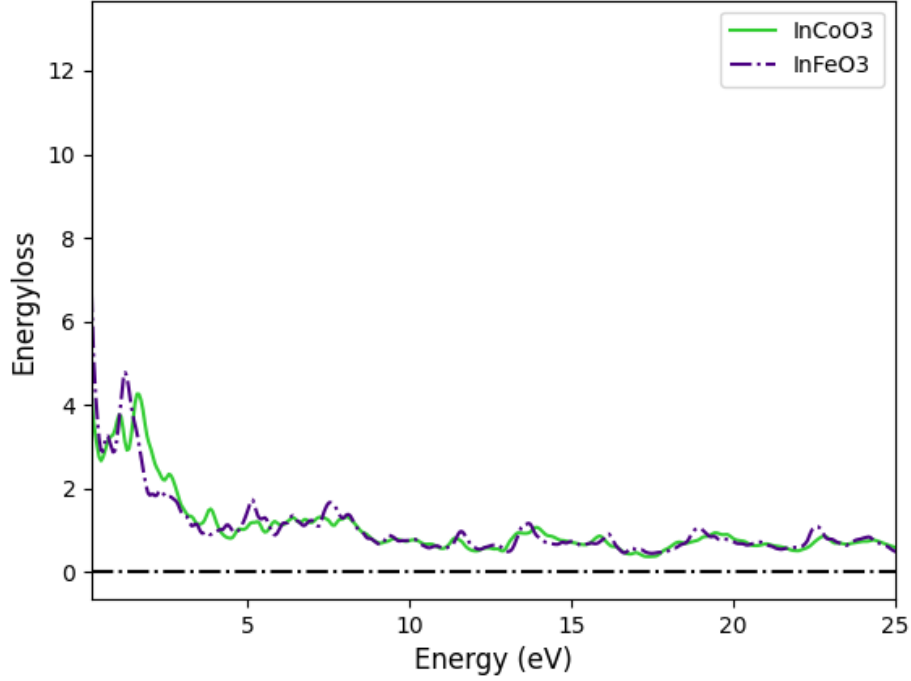


Figure 16: Energyloss spectrum of InCoO3 and InFeO3

5 Conclusion

We performed a study on InCoO3 and InFeO3[2] perovskite cubic materials using DFT simulations for their structural, optical, and dielectric properties. InCoO3 and InFeO3 structures show identical indirect bandgap while InFeO3 shows more magnetic than InCoO3. Fe is a better contender than Co for optical absorption and optical conductivity. Both the material can be an excellent choice for various photovoltaic applications, memory devices, and more. InCoO3 give band-gap Of 0.0017eV and InFeO3 give band-gap of

0.0034eV. So, they are magnetic materials.

References

- [1] Ashish Kumar, Ajay Kumar, and Venkata Krishnan. Perovskite oxide based materials for energy and environment-oriented photocatalysis. *Acs Catalysis*, 10(17):10253–10315, 2020.
- [2] Anton R Chakhmouradian and Patrick M Woodward. Celebrating 175 years of perovskite research: a tribute to roger h. mitchell. *Physics and Chemistry of Minerals*, 41(6):387–391, 2014.
- [3] Stephen J Skinner. Recent advances in perovskite-type materials for solid oxide fuel cell cathodes. *International Journal of Inorganic Materials*, 3(2):113–121, 2001.
- [4] K-I Kobayashi, T Kimura, H Sawada, K Terakura, and Y Tokura. Room-temperature magnetoresistance in an oxide material with an ordered double-perovskite structure. *Nature*, 395(6703):677–680, 1998.
- [5] Koji Fujita, Takahiro Kawamoto, Ikuya Yamada, Olivier Hernandez, Naoaki Hayashi, Hirofumi Akamatsu, William Lafargue-Dit-Hauret, Xavier Rocquefelte, Masafumi Fukuzumi, Pascal Manuel, et al. Linbo3-type infeo3: room-temperature polar magnet without second-order jahn–teller active ions. *Chemistry of Materials*, 28(18):6644–6655, 2016.

- [6] Kieron Burke. Perspective on density functional theory. *The Journal of chemical physics*, 136(15):150901, 2012.
- [7] Anubhav Jain, Geoffroy Hautier, Charles J Moore, Shyue Ping Ong, Christopher C Fischer, Tim Mueller, Kristin A Persson, and Gerbrand Ceder. A high-throughput infrastructure for density functional theory calculations. *Computational Materials Science*, 50(8):2295–2310, 2011.
- [8] Ann E Mattsson, Peter A Schultz, Michael P Desjarlais, Thomas R Mattsson, and Kevin Leung. Designing meaningful density functional theory calculations in materials science—a primer. *Modelling and Simulation in Materials Science and Engineering*, 13(1):R1, 2004.
- [9] Michel Bockstedte, Alexander Kley, Jörg Neugebauer, and Matthias Scheffler. Density-functional theory calculations for poly-atomic systems: electronic structure, static and elastic properties and ab initio molecular dynamics. *Computer physics communications*, 107(1-3):187–222, 1997.
- [10] Kurt Lejaeghere, Gustav Bihlmayer, Torbjörn Björkman, Peter Blaha, Stefan Blügel, Volker Blum, Damien Caliste, Ivano E Castelli, Stewart J Clark, Andrea Dal Corso, et al. Reproducibility in density functional theory calculations of solids. *Science*, 351(6280):aad3000, 2016.

- [11] Jürgen Hafner. Ab-initio simulations of materials using vasp: Density-functional theory and beyond. *Journal of computational chemistry*, 29(13):2044–2078, 2008.
- [12] James E Bear, Tatyana M Svitkina, Matthias Krause, Dorothy A Schafer, Joseph J Loureiro, Geraldine A Strasser, Ivan V Maly, Oleg Y Chaga, John A Cooper, Gary G Borisy, et al. Antagonism between ena/vasp proteins and actin filament capping regulates fibroblast motility. *Cell*, 109(4):509–521, 2002.
- [13] M Reinhard, K Giehl, K Abel, C Haffner, T Jarchau, V Hoppe, BM Jockusch, and U Walter. The proline-rich focal adhesion and microfilament protein vasp is a ligand for profilins. *The EMBO journal*, 14(8):1583–1589, 1995.